

Cite this: *New J. Chem.*, 2011, **35**, 2647–2652

www.rsc.org/njc

PAPER

Activity of carbon electrodes towards oxygen reduction in acid: A comparative study†

Matthew Gara and Richard G. Compton*

Received (in Montpellier, France) 12th July 2011, Accepted 22nd August 2011

DOI: 10.1039/c1nj20612e

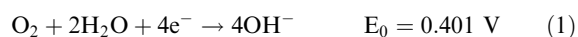
The oxygen reduction reaction (ORR) has been investigated on a variety of carbon substrates, in acidic conditions, including glassy carbon (GC), edge plane pyrolytic graphite (EPPG), basal plane pyrolytic graphite (BPPG) and boron doped diamond (BDD). Along with these macro-sized substrates, a selection of carbon nanotube modified BPPG electrodes have also been examined. These include single walled (SWCNT), bamboo multi walled (B-MWCNT) and hollow multi walled (H-MWCNT) carbon nanotube modified BPPG. Low potential responses for ORR are found for substrates with large quantities of edge plane sites, namely EPPG and MWCNT modified BPPG. Along with being analytically significant in respect of gas sensing, these results have implications for proton exchange membrane (PEM) fuel cell catalyst supports.

Introduction

The reduction of oxygen in aqueous solutions can proceed by two major pathways: A direct four electron pathway and a two electron 'peroxide' pathway.^{1,2} These pathways are further dependant on pH conditions. Both pathways are listed below for both alkaline and acidic conditions.

Direct 4-electron pathway

Alkali



Acid



Peroxide pathway

Alkali



Acid

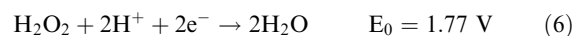


In certain circumstances the peroxide can be further reduced, as shown in eqn (5) and (6)

Alkali



Acid



It is worth noting that summation of the two sequential two electron reductions (involving peroxide) leads to the respective 4 electron reduction (*e.g.* summation of equations 3 + 5 and 4 + 6 are equivalent to eqn (1) and (2) respectively.)

Eqn (2) is the driving force behind proton exchange membrane (PEM) fuel cells^{3,4} and is effected by a catalyst on the cathode. This cathode catalyst is usually comprised of platinum nanoparticles (generally 3 nm in diameter) supported onto a finely divided carbon support (generally 20 nm diameter.) Hydrogen gas, oxidised on the anode, provides the protons required to complete the reaction. These travel through a proton exchange membrane, which is normally a perfluorinated ionomer; the most common of which is Nafion[®].

Whilst the vast majority of oxygen reduction, on platinum, proceeds via the four electron process in eqn (2) a very small percentage follows the peroxide pathway shown in eqn (4). This pathway produces hydrogen peroxide which has the potential to decompose into •OH radicals. These radicals are known to attack the carboxylic end groups (formed during the polymerization process) of the perfluorinated, ionomer chain.⁵

Oxygen reduction on carbon usually proceeds by the more common two electron, peroxide pathway.¹ Whilst there is much literature surrounding this process in alkali,^{6–8} there is significantly less for the process in acidic solutions, relevant to PEM fuel cells. Hence this work is directed solely at oxygen reduction, on carbon, under acidic conditions (specifically aqueous sulphuric acid.) Under these conditions oxygen

Physical and Theoretical Chemistry Laboratory, University of Oxford, South Parks Road, Oxford, OX1 3QZ, United Kingdom.
E-mail: richard.compton@chem.ox.ac.uk

† Electronic supplementary information (ESI) available. See DOI: 10.1039/c1nj20612e

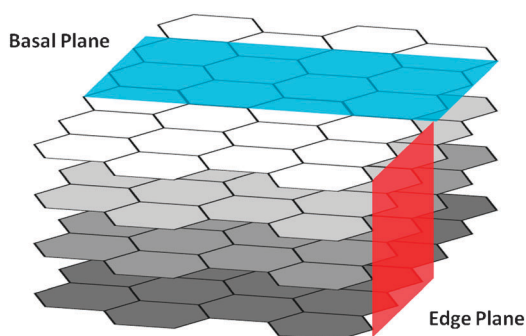


Fig. 1 Schematic diagram showing the relative orientations of the basal and edge planes within a graphitic structure.

reduction is known to progress according to eqn (4) with no further reduction of the peroxide⁹ (eqn (6).)

Carbon electrodes come in a variety of forms,^{10,11} some of which are briefly summarised in the subsequent text. Boron doped diamond (BDD) is a hard material where the carbon atoms are sp^3 hybridised and arranged in a diamond structure, with approximately one atom in a thousand replaced with boron. This creates a hard, conducting, diamond like carbon substrate.¹² Ordered pyrolytic graphite contains ordered layers of sp^2 hybridised carbon stacked 3.35 Å apart. Basal plane pyrolytic graphite (BPPG) electrodes are cut so as to expose the hexagonal plane of the graphite layer. Edge plane pyrolytic graphite (EPPG) is cut perpendicular to BPPG, so as to expose as many graphite sheet ends as possible. A schematic representation of graphite orientations can be seen in Fig. 1. Glassy Carbon (GC) forms at high temperature and pressure and is composed of interlinked strands of graphite forming a random mesh of graphitic ribbons. Carbon nanotubes can be seen as a graphite sheet that has been rolled up to make a tube. Single walled nanotubes (SWCNTs) basically contain only one layer of graphite. As the name suggests multi-walled nanotubes contain several layers. If the tubes are placed one inside the other this is termed a hollow multi-walled carbon nanotube (H-MWCNT.) Bamboo multi-walled carbon nanotubes (B-MWCNTs) are formed at an angle to the propagating axis of the tube, these tubes are 'stacked' to form a bamboo type structure, with the tube closed periodically along the axis. Nanotubes based on chirality also exist, however separation and purification difficulties place these outside the scope of this study. Nitrogen doping of carbon nanotubes has been shown to enhance the rate of oxygen reduction^{13,14} as has the introduction of nitrogen containing species such as FeN_4 porphyrin type moieties.¹⁵

It is worth noting that the electrode kinetics of a redox couple at a graphitic basal plane can be orders of magnitude slower than those of the corresponding edge plane.^{1,16,17} Hence a small quantity of basal planes on an edge plane electrode will make little or no difference whereas a small amount of edge planes on a basal plane electrode can potentially make a big difference¹⁶ to the observed electroactivity. Due to the fact that it is almost impossible to make an electrode consisting purely of basal planes, a certain amount of edge plane sites are to be expected at step edges and grain boundaries, on a basal plane electrode.

The results from this paper will aim to characterise and compare oxygen reduction, in acidic media, across a broad,

but non-exhaustive, range of carbon substrates, which exclude doped graphitic structures.

Experimental

Materials & instrumentation

All carbon nanotubes were acquired from Nanolab inc. Single walled carbon nanotubes (Batch number P0340, containing small amounts of Fe) bamboo multi-walled carbon nanotubes (Batch number BPD30L520-020306, typical EDAX analysis 0.05% S, 0.2% Fe, 30 ± 15 nm diameter, 5–20 μm length) hollow multi-walled carbon nanotubes (Batch number PD30L520-92206, typical EDAX analysis 0.05% S, 0.2% Fe, 30 ± 15 nm diameter, 5–20 μm length) Basal and edge plane pyrolytic graphite electrodes were cut from graphite obtained from le Carbone. Each electrode was cut to 5 mm diameter and mounted in PTFE. Glassy carbon electrodes were obtained from BAS Technical, working diameter 3 mm. Boron doped diamond was obtained from Windsor scientific cut to 5 mm diameter and mounted in PEEK. Oxygen and Nitrogen (oxygen free) were obtained from BOC gasses. All water used was distilled before being passed through a Millipore system. Chloroform was obtained from Fisher Scientific (Batch number C/4920/17-1007754.) Sulphuric acid was of high purity Primar grade, suitable for trace metal analysis (Fisher Scientific Batch number S/9230/PB07-9895337.) All voltammograms were run using a Metrohm Autolab, μAutolab II potentiostat.

Electrode preparation

EPPG electrodes were polished with 1 μm, 0.3 μm and 0.05 μm alumina, with thorough rinsing, with water, and sonicating (2 mins) after each polishing stage. BPPG electrodes were sanded with P1000 abrasive paper, rinsed with water, repeatedly cleaved with adhesive tape and rinsed again. BDD and GC electrodes were polished with 1 μm and 0.1 μm diamond spray with thorough rinsing, with water, and sonicating (2 mins) after each polishing stage.

Carbon nanotube modified electrodes were prepared by drop-casting a dispersion onto a BPPG electrode. This was done by placing 1 mg of the appropriate nanotubes into 5 ml of chloroform and sonicating for 3 sessions of 5 min each, leaving to cool in-between. 20 μl of this black dispersion was then drop-cast onto a freshly prepared BPPG electrode in 4, 5 μl aliquots, leaving the chloroform to evaporate between each casting.

Methods

Voltammograms were run using a saturated calomel reference electrode (SCE) and a platinum mesh counter electrode. Gasses were bubbled through for 25 mins to achieve saturation. The electrode to be tested was first placed into a 0.1 M solution of H_2SO_4 saturated with oxygen. 3 blank voltammograms were then run at 100 $mV s^{-1}$ to equilibrate the electrode and mitigate any effects caused by trapped solvent, such as chloroform from the carbon nanotube drop-casting. Cyclic voltammograms were then run at 10 $mV s^{-1}$, 20 $mV s^{-1}$, 40 $mV s^{-1}$, 100 $mV s^{-1}$, 200 $mV s^{-1}$, 400 $mV s^{-1}$, 800 $mV s^{-1}$, across the scan ranges specified below, rinsing between each voltammogram.

The electrode was then removed and placed into a nitrogen saturated solution of 0.1 M H₂SO₄ and cyclic voltammograms were then run at 10 mV s⁻¹, 20 mV s⁻¹, 40 mV s⁻¹, 100 mV s⁻¹, 200 mV s⁻¹, 400 mV s⁻¹, 800 mV s⁻¹, across the scan ranges specified below, rinsing between each voltammogram.

For EPPG, GC, SWCNT, H-MWCNT and B-MWCNT the potential was scanned from + 0.6 V to -0.8 V for BPPG and BDD the potential was scanned from + 0.6 V to -1.0 V and + 0.6 V to -1.3 V respectively

Results and discussion

The results for the investigation into oxygen reduction on carbon substrates have been split into two main categories. Results relating to the unmodified carbon, macroelectrodes will be dealt with separately to the results concerning the carbon nanotube modified BPPG electrodes.

Carbon Macroelectrodes

Cyclic voltammograms were measured for a range of scan rates, in both O₂ and N₂ saturated H₂SO₄, detailed in the experimental section. While the majority of experiments in O₂ saturated solution gave a response for oxygen reduction, those of the control experiments in N₂ saturated solution (see ESI†) gave very little response with most nothing except a response for the breakdown of solvent. Fig. 2 summarises the results acquired on unmodified carbon macroelectrode substrates, in O₂ saturated 0.1 M H₂SO₄. It is clear from Fig. 2 that BDD gives little or no response to oxygen reduction. This agrees with the work of Yano *et al.*¹⁸ who found that oxygen reduction on BDD could only be initiated by pretreatment at positive potentials greater than about + 1.4 V vs. Ag/AgCl. This was attributed to sp² hybridised carbon species becoming oxidised and mediating oxygen reduction, with the most likely location for the sp² species being the grain boundaries of the, sp³, diamond structure.

The response obtained from glassy carbon towards oxygen reduction occurred very close to the breakdown of solvent, convoluting the signal. Although comparison with the corresponding results for the nitrogen saturated solution clearly indicate some response towards oxygen reduction. Signals for glassy carbon have been corrected to account for the difference in electrode area.

Fig. 2 also shows that the analytical response of EPPG is better than that of any other electrode substrate. In particular the current voltage curve for oxygen reduction on EPPG is shifted around + 450 mV higher than for BPPG. This fits with previous investigations which have found the electrode kinetics on the basal plane to be far slower than those of edge plane sites¹⁶ (possibly 7 orders of magnitude slower.) The results for EPPG are shown in more detail in Fig. 3a. Fig. 3b shows the corresponding Randles Ševčík plot of the data in Fig. 3a. The equation used for this plot is shown in eqn (7).

$$I_{peak} = -0.496\sqrt{(n' + \alpha'_n)nFA[O_2]}\sqrt{\frac{FvD}{RT}} \quad (7)$$

where I_{peak} is the peak current, n' is the number of electrons transferred before the rate determining electron transfer, α'_n is the electron transfer coefficient of the rate determining step,

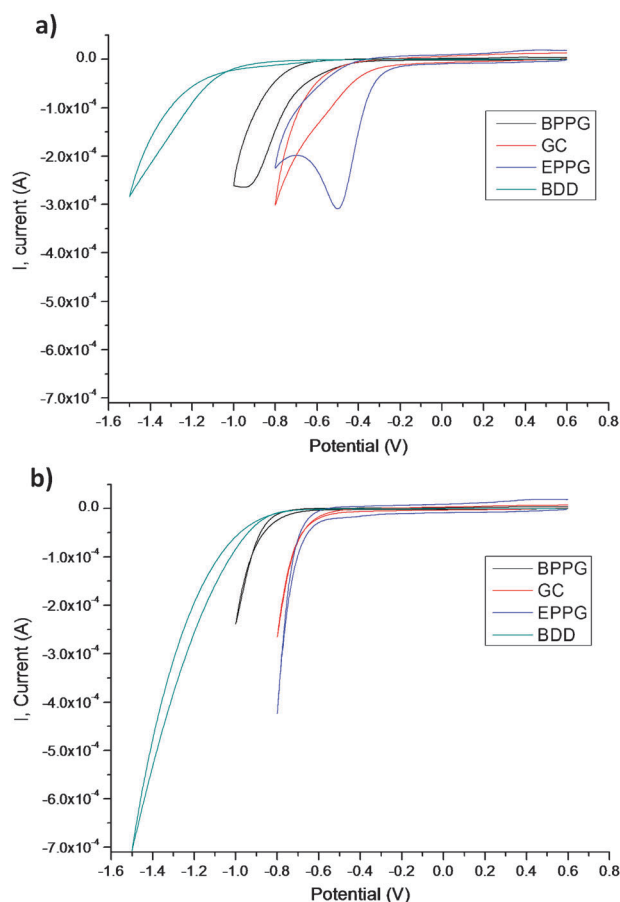


Fig. 2 Cyclic voltammograms taken at 400 mV s⁻¹ using BPPG, EPPG, GC and BDD electrodes in (a) O₂ saturated 0.1 M H₂SO₄ solution and (b) N₂ saturated 0.1 M H₂SO₄ solution. The potential was swept in a negative direction from 0.6 vs. saturated calomel electrode (SCE).

n is the number of electrons transferred, F is the Faraday constant, A is the area of the electrode, $[O_2]$ is the oxygen concentration, T is the absolute temperature, R is the gas constant and ν is the scan rate.

Tafel analyses (eqn (8)) on the EPPG results give an average value for $(n' + a')$ of 0.4; an example Tafel plot can be seen in Fig. 4. Using this value along with $[O_2] = 1.3 \text{ mM}$ ¹⁹ and $n = 2$, a diffusion coefficient of $2.1 \times 10^{-5} \text{ cm}^2 \text{ s}^{-1}$ was obtained for oxygen. This value shows good agreement with the value of $2.0 \times 10^{-5} \text{ cm}^2 \text{ s}^{-1}$ obtained from interpolating data from reference 20.

$$\frac{\partial \ln I}{\partial E} = \frac{(n' + \alpha'_n)F}{RT} \quad (8)$$

Nanotube modified electrodes

All nanotubes were immobilised onto the surface using a simple dropcasting technique using chloroform dispersions. The hydrophobicity of all the carbon nanotube modified electrodes was very apparent, with all the nanotube modified electrodes forming beads of water rather than wetting the surface. Again the results in N₂ saturated solution (see ESI†) showed little or no response except for the breakdown of solvent.

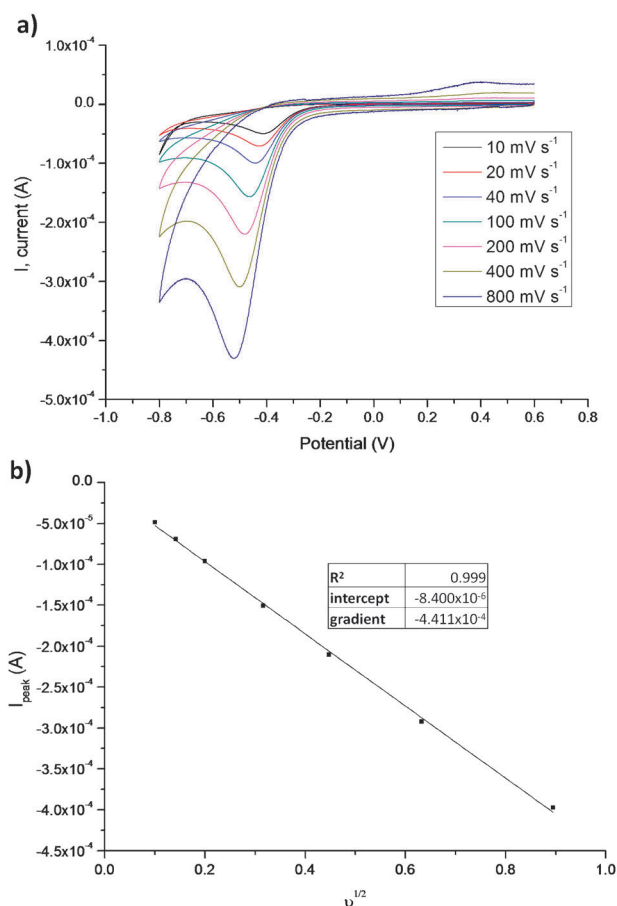


Fig. 3 (a) Cyclic voltammograms taken at scan rates of 800, 400, 200, 100, 40, 200, 10 mV s^{-1} , on a 0.5 cm EPPG electrode in an O_2 saturated 0.1 M H_2SO_4 solution. The potential was swept from 0.6 to -0.8 V vs. saturated calomel electrode (SCE) (b) Corresponding Randles Sevcik plot (using eqn (7)) for the data shown for EPPG.

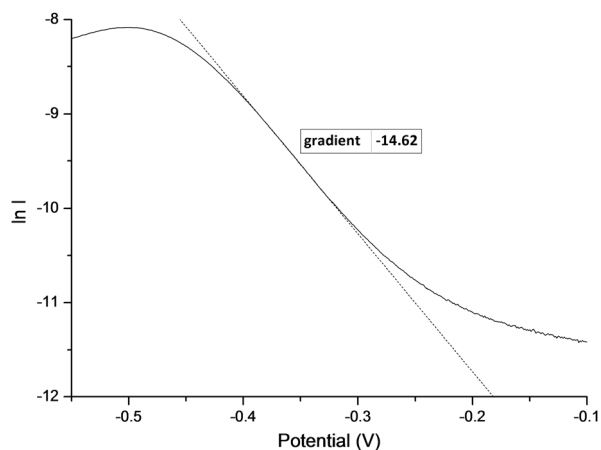


Fig. 4 An example Tafel plot, showing the 'Tafel region', used to calculate the value for $(n' - \alpha)$ for the 400 mV s^{-1} scan shown in Fig. 3a. The line used for Tafel analysis can be seen as a dashed line with a gradient of -14.62 . This is an example of 7 such plots used to give an average value for $(n' - \alpha)$.

Results obtained using carbon nanotube modified BPPG electrodes, in O_2 saturated solution, are summarised in Fig. 5. A ca. 320 mV difference was found between the current

voltage curves for hollow and bamboo carbon nanotubes, with the curve for bamboo nanotubes shifted to higher potential. This broadly agrees with the work of Matsubara *et al.*²¹ who found a 312 mV difference in 'onset potentials'. This difference is likely to be attributable to the fact that the bamboo structured nanotubes have a significantly larger proportion of edge plane sites per unit length, compared with the hollow structured nanotubes, where edge plane sites have a tendency to appear only at the ends of the nanotube.

Of particular interest, and the most noticeable feature of Fig. 5, is that only the hollow nanotube (H-MWCNT) gave an analysable peak. Further analysis, which will be shown in more detail later, reveals that this is partly due to the porous nature of the H-MWCNT modified electrode. A full set of results for the H-MWCNT modified electrode is shown in Fig. 6.

Fig. 7a shows a log peak current against log scan rate plot for calculated, theoretical peak currents and for experimental, peak currents obtained using the H-MWCNT modified electrode. Calculated peak currents were obtained from eqn (7) using $[\text{O}_2] = 1.3 \text{ mM}$,¹⁹ $(n' + \alpha') = 0.5$, $n = 2$ and $D = 2.0 \times 10^{-5} \text{ cm}^2 \text{ s}^{-1}$.²⁰ If the electron transfer takes place in the solution this plot should give a linear relationship, with a

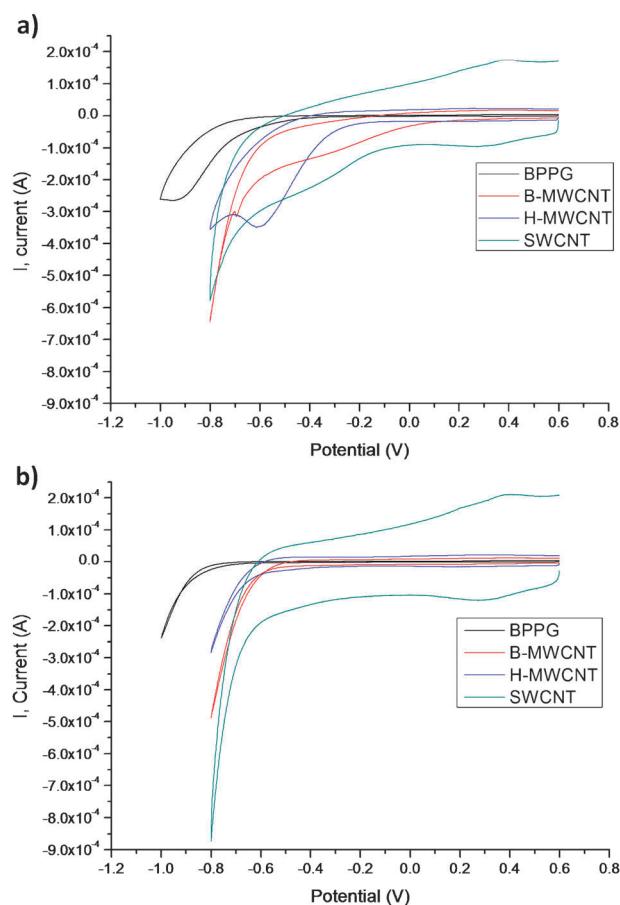


Fig. 5 Cyclic voltammograms taken at 400 mV s^{-1} , using SWCNT, B-MWCNT and H-MWCNT modified BPPG electrodes, in (a) O_2 saturated 0.1 M H_2SO_4 solution and (b) N_2 saturated 0.1 M H_2SO_4 solution. The potential was swept in a negative direction from 0.6 vs. saturated calomel electrode (SCE).

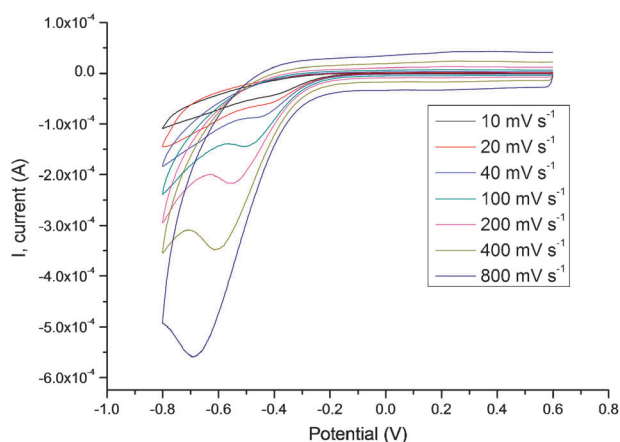


Fig. 6 Cyclic voltammograms taken at scan rates of 800, 400, 200, 100, 40, 200, 10 mV s^{-1} , on a H-MWCNT modified BPPG electrode in an O_2 saturated 0.1 M H_2SO_4 solution. The potential was swept from 0.6 to -0.8 V vs. saturated calomel electrode (SCE.)

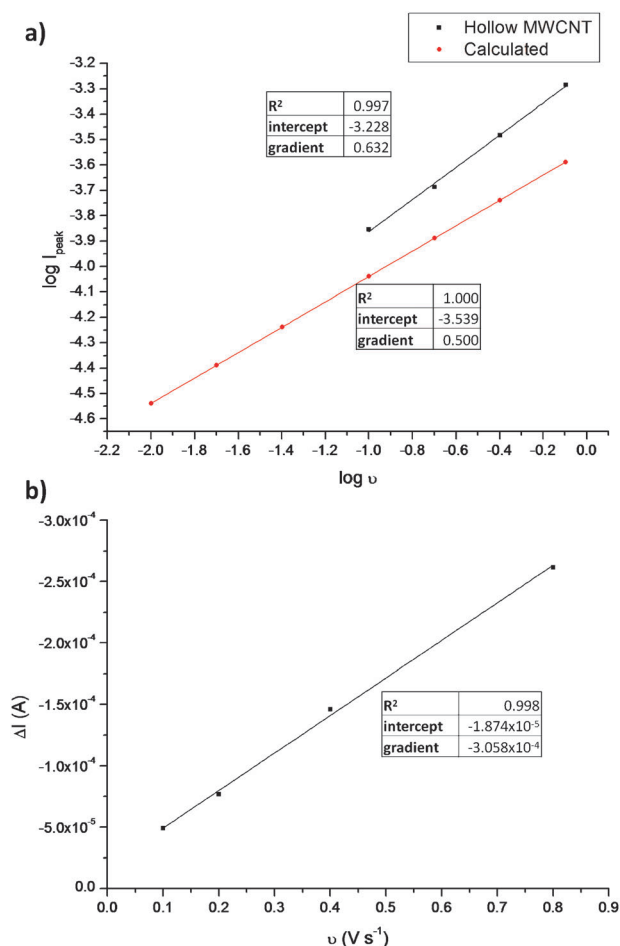


Fig. 7 (a) \log of the peak current ($\log I_{\text{peak}}$) plotted against \log scan rate ($\log \nu$). The black line shows the calculated peak currents from eqn (7) whereas the red line shows the peak currents obtained from H-MWCNT electrodes. (b) The residual current (ΔI) plotted against scan rate (ν).

gradient of 0.5, according to eqn (7). We can see from Fig. 7a that while the data using calculated, theoretical, currents (for semi-infinite diffusion) gives a gradient of 0.5, the experimental

data using the HMWCNT modified electrode gives a gradient of 0.63, indicating that there is an additional contribution to the current.

Further to Fig. 7a, Fig. 7b shows the difference in current (ΔI), between the calculated peak currents and the ones acquired for the H-MWCNT modified electrode, plotted against scan rate. This graph shows a linear relationship which intercepts very close to the origin, suggesting that thin layer diffusion within the porous layer is contributing to the signal. This is in keeping with previous studies on multiwalled carbon nanotubes^{22,23} and other porous layer systems,^{24,25} which show that as the thickness of a porous electrode increases, the contribution from thin-layer diffusion also increases. This current contribution from thin-layer diffusion was found to be linearly dependant on scan rate.

On the basis of the solubility of oxygen in water and its diffusion coefficient the peaks shown in Fig. 3a for oxygen reduction on EPPG are qualitatively consistent with a value of $n = 2$ (see above) and hence the formation of hydrogen peroxide (*cf.* eqn (4).) In comparison the peak current on BPPG is a little reduced and occurs at higher overpotential. Hence this signal likely does not reflect a decrease in the n value but rather the fact that the electrolysis only occurs at edge plane like defects on the BPPG surface (*i.e.* the electrode is heterogeneous) with the basal plane terraces contributing little to the current.^{1,16,17} The peak current response for H-MWCNT is close to that seen for EPPG but quantitative analysis is precluded because of the contribution of mass transport within the porous H-MWCNT coat,^{22,23} that said the closeness in size of the signal to that seen on the EPPG electrode (of the same geometric area) suggests that $n = 2 \pm 0.2$. The Single walled (SWCNT) and the bamboo multi walled (B-MWCNT) carbon nanotube modified electrodes show no well defined reduction signal (Fig. 5a) precluding analysis of the number of electrons transferred.

Being comprised entirely of sp^3 carbon atoms born doped diamond does not possess any edge plane character and it is clear to see from Fig. 2a that it gives a negligible current response towards oxygen reduction in sulphuric acid. Likewise the basal plane of graphite would also be expected to show little/no edge plane character and whilst some current response can be seen for BPPG, this can be ascribed to the inevitable heterogeneity of the surface, with some edge plane like defects being present. Being orientated perpendicular to the basal plane (*cf.* Fig. 1) EPPG affords the maximum density of edge plane sites per unit area; in turn EPPG gives the best analytical response of all the substrates tested. Glassy carbon is thought to have no well defined edge plane sites. This is reflected in the results, with the nature of the oxygen reduction signal being closer to BPPG than EPPG.

In comparison to Hollow multiwalled carbon nanotubes (H-MWCNT) bamboo multi walled carbon nanotubes (B-MWCNT) contain many edge plane like sites along the axis of the entire tube rather than purely at the ends. This distinct difference in structure (the number of edge plane sites) is reflected in significantly less overpotential being required to enact oxygen reduction on bamboo compared to hollow multi walled carbon nanotube modified electrodes.

Conclusions

From the results presented here it is possible to see that graphitic structures give a better analytical response to oxygen reduction than the cubic diamond structure of BDD. It is also possible to see that, within those graphitic structures, the substrates with a large number of edge plane sites have a higher activity towards oxygen reduction and therefore a higher tendency to produce H₂O₂ if used as a catalyst support in a PEM fuel cell. It is therefore favourable to decrease the number of edge plane sites in carbon catalyst supports for PEM fuel cells in order to increase efficiency and reduce membrane degradation from hydrogen peroxide attack.

Acknowledgements

Matthew Gara would like to thank EPSRC and Johnson Matthey for an Industrial CASE award.

References

- 1 in *Comprehensive Treatise of Electrochemistry, Vol 7 &: Kinetics and Mechanisms of Electrode Processes*, ed. B. Conway, J. Bockris, E. Yeager, S. Khan and R. White, Plenum Press, New York, 1983, vol. 7, pp. 301–398.
- 2 E. Yeager, *Electrochim. Acta*, 1984, **29**, 1527–1537.
- 3 S. Litster and G. McLean, *J. Power Sources*, 2004, **130**, 61–76.
- 4 J. Larminie and A. Dicks, *Fuel Cell systems Explained*, Wiley, 2nd edn, 2003.
- 5 D. E. Curtin, R. D. Lousenberg, T. J. Henry, P. C. Tangeman and M. E. Tisack, *J. Power Sources*, 2004, **131**, 41–48.
- 6 E. Yeager, *J. Mol. Catal.*, 1986, **38**, 5–25.
- 7 B. Sljukic, C. E. Banks and R. G. Compton, *J. Iranian Chem. Soc.*, 2005, **2**, 1–25.
- 8 H. H. Yang and R. L. McCreery, *J. Electrochem. Soc.*, 2000, **147**, 3420–3428.
- 9 in *Comprehensive Treatise of Electrochemistry, Vol 4: Electrochemical Materials Science*, ed. B. Conway, J. Bockris, E. Yeager, S. Khan and R. White, Plenum Press, New York, 1981, vol. 4, pp. 486–489.
- 10 C. E. Banks and R. G. Compton, *Analyst*, 2006, **131**, 15–21.
- 11 R. L. McCreery, *Chem. Rev.*, 2008, **108**, 2646–2687.
- 12 R. G. Compton, J. S. Foord and F. Marken, *Electroanalysis*, 2003, **15**, 1349–1363.
- 13 K. Gong, F. Du, Z. Xia, M. Durstock and L. Dai, *Science*, 2009, **323**, 760–764.
- 14 N. Alexeyeva, E. Shulga, V. Kisand, I. Kink and K. Tammeveski, *J. Electroanal. Chem.*, 2010, **648**, 169–175.
- 15 D. H. Lee, W. J. Lee, W. J. Lee, S. O. Kim and Y.-H. Kim, *Phys. Rev. Lett.*, 2011, **106**, 175502.
- 16 C. E. Banks, T. J. Davies, G. G. Wildgoose and R. G. Compton, *Chem. Commun.*, 2005, 829–841.
- 17 C. C. M. Neumann, C. Batchelor-McAuley, C. Downing and R. G. Compton, *Chem.–Eur. J.*, 2011, **17**, 7320–7326.
- 18 T. Yano, E. Popa, D. A. Tryk, K. Hashimoto and A. Fujishima, *J. Electrochem. Soc.*, 1999, **146**, 1081–1087.
- 19 T. N. Das, *Ind. Eng. Chem. Res.*, 2005, **44**, 1660–1664.
- 20 P. Han and D. M. Bartels, *J. Phys. Chem.*, 1996, **100**, 5597–5602.
- 21 K. Matsubara and K. Waki, *Electrochim. Acta*, 2010, **55**, 9166–9173.
- 22 M. C. Henstridge, E. J. F. Dickinson, M. Aslanoglu, C. Batchelor-McAuley and R. G. Compton, *Sens. Actuators, B*, 2010, **145**, 417–427.
- 23 M. J. Sims, N. V. Rees, E. J. F. Dickinson and R. G. Compton, *Sens. Actuators, B*, 2010, **144**, 153–158.
- 24 I. Streeter, G. G. Wildgoose, L. D. Shao and R. G. Compton, *Sens. Actuators, B*, 2008, **133**, 462–466.
- 25 L. Xiao, G. G. Wildgoose and R. G. Compton, *Sens. Actuators, B*, 2009, **138**, 524–531.